Diffusion Tensor MRI and MR Spectroscopy in long lasting upper motor neuron involvement in Amyotrophic Lateral Sclerosis

F. LOMBARDO[1], F. FRIJIA[1], P. BONGIOANNI[2], R. CANAPICCHI[1],
F. MINICHILLI[3], F. BIANCHI[3], H. HLAVATA[1], B. ROSSI[2], D. MONTANARO[1]

[1] *Fondazione CNR/Regione Toscana, U.O.S. Neuroradiologia, Pisa, Italy;*
[2] *Neurological Rehabilitation, University of Pisa, Italy;*
[3] *Institute of Clinical Physiology, CNR, Pisa, Italy*

A B S T R A C T

Upper motor neuron (UMN) dysfunction in Amyotrophic Lateral Sclerosis (ALS) is not easy to identify clinically: Diffusion Tensor Imaging (DTI) and single-voxel Magnetic Resonance Spectroscopy (H-MRS) can identify markers of UMN involvement. The aim of this study was to correlate brain DTI and MRS data with clinical parameters in ALS patients (PALS).
We studied 32 PALS using Magnetic Resonance Imaging. The subjects were subdivided into definite/probable (D/P) and possible/suspected (P/S). DTI indices included Fractional Anisotropy (FA) and averaged Apparent Diffusion Coefficient (avADC). Anatomical areas were sampled by positioning regions of interest along cortico-spinal tracts, from the precentral cortex to the bulb. H-MRS voxels were localized bilaterally in precentral regions.
D/P-PALS showed significantly lower FA values than healthy controls in almost all regions, whereas P/S-PALS FA values were significantly lower only in the left precentral gray matter (GM), right precentral white matter (WM), cerebral peduncles (CP), left hemipons, and left bulbar pyramid (BP).
Significantly higher avADC values were observed in the D/P-PALS right precentral GM, precentral WM, right semioval center-posterior limb of the internal capsule (SC-PLIC), and left CP; and in the precentral WM, right SC-PLIC, left CP, and right hemipons of P/S-PALS.
With increasing disability, only D/P-PALS showed significantly reduced FA values in the left precentral WM and hemipons, and increased avADC values in the precentral WM.
Significantly lower N-acetylaspartate (NAA)/creatine-phosphocreatine complex (Cr) and higher choline (Cho)/Cr and myoinositol (mI)/Cr ratios were found in D/P-PALS, while only higher Cho/Cr and mI/Cr ratios were found in P/S-PALS.
Our data highlight the usefulness of DTI and H-MRS in assessing UMN involvement. Given FA sensitivity and specificity, despite the small number of PALS, our findings support its use as a diagnostic marker in D/P-PALS.

Key words
Amyotrophic Lateral Sclerosis • Diffusion Tensor Imaging • Magnetic Resonance Spectroscopy

Introduction

Amyotrophic Lateral Sclerosis (ALS) is a neuro-degenerative disease progressively involving the cortex, brainstem and spinal cord motor neurons. Both upper motor neuron (UMN) and lower motor neuron (LMN) dysfunctions are required for an ALS diagnosis (Brooks et al., 2000). Whereas LMN degeneration can be demonstrated electro-myographically, there are no objective markers of UMN involvement (Ellis et al., 2001), which would be very useful in neurological practice as well as

Corresponding Author: Domenico Montanaro, Fondazione CNR/Regione Toscana, U.O.S. Neuroradiologia, via G. Moruzzi 1, I 56124 Pisa, Italy - Tel.: +39 050 3152824 - Fax: +39 050 3152166 - Email: domont@ifc.cnr.it

in clinical trials (Sach et al., 2004). Neuroimaging in ALS is currently performed in order to rule out other curable illnesses, such as immuno-mediated, metabolic, toxic or drug-induced. Cortico-spinal tract (CST) involvement has been studied using Magnetic Resonance Imaging (MRI) with variable results. Changes observed were neither sensitive nor specific (Ellis et al., 2001); however, a recent report highlighted a good correlation with ALS (Ghaham et al., 2004).

Attention has been more recently focussed on Diffusion Tensor Imaging (DTI). DTI indices include mean diffusivity, which measures the magnitude of direction-independent water diffusion (avADC), and fractional anisotropy (FA), which quantifies water diffusion directionality (Pierpaoli et al., 1996). Such quantitative markers are useful in studying micro-structural and functional white matter (WM) integrity since they detect the preferential water diffusion along fiber tracts.

In recent years many authors (Ellis et al. 1999; Toosy et al., 2003; Ghaham et al., 2004; Hong et al., 2004; Yin et al., 2004; Cosottini et al., 2005; Ciccarelli et al., 2006; Wang et al., 2006; Blain et al., 2007; Mitsumoto et al., 2007; Sage et al., 2007; Thivard et al., 2007; Iwata et al., 2008) have used DTI to study patients affected by ALS (PALS), showing significantly lower FA at different CST levels compared to healthy controls.

Some authors found in few regions significant correlations between clinical disabilities, length of illness and diffusion indices. Ellis et al. (1999) and Cosottini et al. (2005) identified a significant correlation between severity and length of illness, lower FA values and higher avADC values in the internal capsule (IC). Still in the IC, Wang et al. (2006) reported an opposite correlation between FA values and length or severity of illness. Exploring the pyramid tract between the WM and the IC, Sage et al. (2007) observed an opposite correlation between FA and clinical disability.

H-MRS provides metabolic markers of UMN involvement (Yin et al., 2004). Spectrum is achieved from a volume of interest specifically chosen to include the diseased tissue, using single voxel samples. N-acetylaspartate (NAA), choline (Cho), creatine-phosphocreatine complex (Cr) and myoi-nositol (mI) resonances are identified in accordance with their spectral position, and expressed in terms of standard-related frequency shifts in parts per million (ppm).

Decreased NAA/Cr ratios and increased mI/Cr and Cho/Cr ratios in PALS have been reported, with both single- and multiple-voxel techniques (Gredal et al., 1997; Bowen et al., 2000; Suhy et al., 2002; Yin et al., 2004; Karla et al., 2006), although some authors have reported no significant differences between PALS and healthy subjects (Ken et al., 2001). On the other hand, Kalra et al. (2006) found that NAA/mI ratios were significantly more decreased compared to NAA/Cr ratios.

Over the last few years several spectroscopic studies have quantified absolute metabolite concentrations in ALS and other neurological diseases (Gredal et al., 1997; Pohl et al., 2001; Dixon et al., 2002; Isobe et al., 2002; Schubert et al., 2002; Fernando et al., 2004; Traber et al., 2006). Gredal et al. (1997) found a significantly decreased absolute NAA concentration in the primary motor cortex of PALS when compared with that of healthy controls. Pohl et al. (2001) studied both absolute metabolite concentrations and their ratios, and reported reduced amounts of NAA and NAA/Cho ratios in the motor cortex.

The aim of our study was to assess water diffusion changes in PALS with a long lasting disease from the prerolandic cortex along the pyramidal tracts down to the brainstem (by DTI). In addition, the aim was to examine metabolic changes in the pre-rolandic regions (by H-MRS), in order to more precisely detect markers of UMN involvement, already investigated in previous studies, but not in such a systematic way, and to establish correlations with clinical data, which until now have been reported only sporadically.

Subjects and methods

Subjects

Thirty two PALS were enrolled at the Neurorehabilitation Unit (Neuroscience Dept, University of Pisa): 13 had definite/probable (D/P)-ALS (6 females and 7 males; mean age ± SD: 54 ± 10 years; mean illness duration ± SD: 39 ± 27 months) and 19 possible/suspected (P/S)-ALS (5 females and 14 males; mean age ± SD: 60 ± 10 years; mean illness duration: 35 ± 26 months) (Table I), according to the El Escorial criteria (World Federation of neurology

Patients	Sex	Age (yrs)	Disease Duration (months)	El Escorial Classification	Disease Severity (score ALSFRS)	Rapidity of Disease Progression	UMN and/ or LMN Involvement
1	M	61	16	P/S	35	0.022	UMN-LMN
2	F	64	54	P/S	32	0.013	UMN-LMN
3	M	60	29	D/P	31	0.033	UMN-LMN
4	M	63	28	P/S	38	0.008	LMN
5	M	52	9	D/P	35	0.038	UMN-LMN
6	F	64	12	D/P	26	0.069	UMN-LMN
7	M	47	20	P/S	36	0.031	LMN
8	F	53	7	P/S	35	0.049	UMN
9	M	44	78	P/S	35	0.005	UMN-LMN
10	F	57	62	D/P	31	0.012	UMN-LMN
11	M	57	61	P/S	12	0.040	LMN
12	M	50	116	D/P	17	0.210	UMN-LMN
13	F	74	32	P/S	24	0.046	LMN
14	M	46	41	D/P	29	0.025	UMN-LMN
15	M	73	78	P/S	19	0.021	UMN-LMN
16	M	54	14	P/S	38	0.180	UMN
17	M	60	23	D/P	40	0.000	UMN-LMN
18	F	77	10	P/S	34	0.028	LMN
19	F	32	59	D/P	13	0.038	UMN-LMN
20	M	48	68	P/S	28	0.014	UMN-LMN
21	M	64	60	P/S	23	0.024	UMN-LMN
22	M	48	31	D/P	27	0.035	UMN-LMN
23	M	75	36	P/S	28	0.029	LMN
24	F	58	35	D/P	20	0.053	UMN-LMN
25	M	62	12	P/S	36	0.046	LMN
26	M	62	32	P/S	39	0.003	LMN
27	F	60	44	D/P	26	0.026	UMN-LMN
28	F	60	26	D/P	37	0.009	UMN-LMN
29	M	52	82	P/S	26	0.014	UMN-LMN
30	M	65	25	D/P	23	0.046	UMN-LMN
31	M	64	10	P/S	33	0.053	UMN-LMN
32	F	51	86	P/S	34	0.006	UMN-LMN

Table I. - Details of patients with ALS.

P/S: possible/suspected ALS; D/P: definite/probable ALS; Rapidity of disease progression: 40-ALSFRS score/disease duration; UMN: Upper Motor Neuron; LMN: Lower Motor Neuron.

Research Group, 1994; Brooks et al., 2000). These PALS were subdivided into possible (P) or suspected (S) on the basis of the 1994 El Escorial classification. Since more recent classification criteria do not include S-PALS (with clinical involvement of LMN only), such cases (7 males and 1 female) were also analysed separately. Each patient was scored according to the ALS Functional Rating Scale, ALSFRS (Cedarbaum et al., 1997), to assess disease severity: lower scores correspond to higher clinical impairment. The PALS were arbitrarily subdivided into three groups (Group I: scoring from 31 to 40; Group II: from 21 to 30; Group III: below 21). For each subject, disease progression was also determined using the following formula (Ellis et al., 1999):

$$Rapidity\ of\ disease\ progression = \frac{(40 - ALSFRS\ score)}{disease\ duration\ (months)}$$

Nineteen healthy controls with normal MRI were studied (4 females and 15 males; mean age ± SD: 54 ± 11 years). Informed consent was obtained from all subjects.

Neuroimaging methods

All patients and controls underwent MRI brain scans (1.5 T GE Signa Excite™ HD, Milwaukee, USA) at the MRI laboratory of the Institute of Clinical Physiology-National Research Council in Pisa.

The MRI protocol followed axial FSE (Fast Spin echo) T2 (TR: 3.500 ms, TE: 102 ms; acquisition matrix: 192x256; FOV: 240 mm; 24 axial contiguous slices, 4-mm thick and 1-mm gap), coronal and axial FLAIR (Fluid Attenuation Inversion Recovery) (TR: 10.000 ms, TI: 2.600 ms; 24 contiguous slices, 4-mm thick and 1-mm gap) conventional images, evaluated blindly and independently by two trained neuroradiologists (FL and DM).

The DTI was performed using single-shot EPI (Echo Planar Image) on an axial plane (TR: 10.000 ms, TE: 88.8 ms; BW: 109 kHz; acquisition matrix: 128x128; FOV: 240 mm; b-value 0 and 1.000 s/mm (Ellis et al., 2001); 24 contiguous slice, 4-mm thick and 1-mm gap), with 25 different gradient directions and tensor reconstruction to get isotropy and anisotropy maps (acquisition time: 5.24 min). DTI images were processed at a workstation (Advantage Windows, GE Medical System, version 4.1), using commercial software (Functool, GE Medical System) and applying a correction for any distortions caused by eddy-currents and micromovements (stretch, translation and shear). By manually defining individual regions of interest (ROI$_s$), FA and average Apparent Diffusion Coefficient (avADC, measuring mean diffusivity) values were obtained on both sides in 1, 2 or 3 consecutive slices, taking into account the rostro-caudal CST direction, bilaterally at the level of prerolandic gray matter (GM) and WM (3 slices), semioval center-posterior limb of internal capsule (SC-PLIC, 1-3 slices), cerebral peduncle (CP) and pons (2 slices respectively), and bulbar pyramid (BP, 1 slice). To locate the ROI$_s$ the b = 0 images of DTI acquisition (as T2 anatomical reference) were visualized. The dimensions of the ROI$_s$ were calibrated on the knee of the internal capsule (IC) (about 33 mm^2, 17.6 pixels), and used for all the regions under study, apart from CP$_s$, pons and BP$_s$ where they were reduced (25 mm^2, 13.3 pixels) to

limit the so-called "partial volume effect" with the cerebrospinal fluid (CSF), due to physiological CST thinning in the brainstem. ROI$_s$ positioning was performed by FL and repeated independently by DM to test measurement reproducibility.

H-MRS was performed by sampling rolandic regions using a single-voxel technique (acquisition time: 5.04 min) with the short TE PRESS (Point Resolved Spectroscopy Sequence) sequence (TR: 2000 ms, TE: 30, FOV: 260 mm, voxel: 15x15x15 mm^3), to get metabolic NAA, Cho and ml peaks, each referred to the Cr peak. Orthogonal images (axial FSE T2, coronal FLAIR and sagittal scout) were used to position volumes of interest. To define a peak table for NAA, Cho, Cr and mI, data were processed using SAGE software 7.0 (GE Medical System).

The total scan time for DTI and H-MRS (both rolandic regions) was 15.32 min.

Statistical analysis

PALS data obtained from the non-structural MRI were compared with the controls. PALS data were cross-compared according to age, sex, diagnosis, clinical disability, progression, and illness duration. A comparison between two independent sample means was carried out using a non-parametric Wilcoxon-Mann-Whitney test; comparisons between more than two means were performed by non-parametric variance analysis. Correlations between MRI data, age, clinical disability and disease progression were evaluated using the non-parametric Spearman (ρ) coefficient. Differences were considered significant for $p < 0.05$.

Test discriminant efficacy was carried out using the Receiver Operating Characteristic (ROC) curve. The area under the ROC curve (AUC) was used to provide a measure of the test's performance. The choice of test with a good performance was based on the following criterion: AUC > 0.8 and lower limit of AUC confidence range > 0.7, according to Swets's classification (Swets, 1998). The cut-off chosen maximized both sensitivity and specificity, namely the highest point on the left of the ROC curve.

The research received prior approval from an internal institutional review body and informed consent was obtained from all the patients and volunteers.

Results

Patients vs. controls

FA and avADC means in specific PALS and control brain regions are shown in Table II.

FA

In D/P-PALS *vs.* controls comparison, lower mean values in all regions, with statistical significance in the left precentral GM, bilaterally precentral WM, bilaterally CP_s and left BP ($p < 0.001$); right BP ($p < 0.01$); right GM and right SC-PLIC ($p < 0.05$) were found (Fig. 1A and Table II).

In P/S-PALS *vs.* controls comparison, overall lower mean values, with statistical significance in the left precentral GM and bilaterally CP_s ($p < 0.001$); right precentral WM, left hemipons and left BP ($p < 0.05$) were found (Fig. 1B and Table II). In S-PALS *vs.* controls: overall lower mean values, with statistical significance in the left precentral GM ($p < 0.01$) and CP_s (bilaterally $p < 0.05$).

avADC

Comparing D/P-PALS *vs.* controls, significantly higher mean values right precentral WM ($p < 0.001$); right SC-PLIC ($p < 0.01$); in right precentral GM, left precentral WM and left CP ($p < 0.05$) were found (Fig. 2A and Table II).

In P/S-PALS *vs.* controls comparison significantly higher mean values in the right precentral WM, right SC-PLIC and left CP ($p < 0.01$); left precentral WM and right hemipons ($p < 0.05$) were found (Fig. 2B and Table II). In S-PALS *vs.* controls: significantly higher mean values only in the right precentral WM ($p < 0.05$).

Spectroscopy

Comparing D/P-PALS *vs.* controls, on both sides, significantly lower NAA/Cr ratio values ($p < 0.05$ bilaterally), higher mI/Cr ($p < 0.01$ bilaterally) and Cho/Cr ($p < 0.05$ bilaterally) ratio values (Fig. 3A and Table III).

In P/S-PALS *vs.* controls, higher mI/Cr ratio values on the left-hand side ($p < 0.05$) and Cho/Cr ratio values on both sides ($p < 0.01$) (Fig. 3B and Table III). In S-PALS *vs.* controls, significantly higher mI/Cr ($p < 0.05$) and Cho/Cr ($p < 0.05$) ratio values on the right-hand side.

Clinical disability

With increasing disability, there were reduced mean FA values only in D/P-PALS in the left precentral WM and left hemipons ($p < 0.05$) (Fig. 4), and increased mean avADC values in the precentral WM ($p < 0.05$ right; $p \leq 0.01$ left) (Fig. 5).

Table II. - Means ± standard deviations and statistically significant p-values (if not = ns) for FA and avADC measurements in ASL D/P and P/S patients and controls.

| Regions of interest	FA values					ADC values (mm²/s x 10⁻⁴)				
	Controls n = 19	D/P Patients n = 13	p < values	P/S Patients n = 19	p < values	Controls n = 19	D/P Patients n = 13	p < values	P/S Patients n = 19	p < values
Precentral GM R	0.28 ± 0.04	0.24 ± 0.03	0.05	0.25 ± 0.05	ns	7.98 ± 1.22	8.74 ± 0.93	0.05	8.39 ± 0.92	ns
Precentral GM L	0.28 ± 0.04	0.23 ± 0.03	0.001	0.24 ± 0.03	0.001	8.05 ± 1.09	8.71 ± 1.15	ns	8.50 ± 0.95	ns
Precentral WM R	0.47 ± 0.05	0.38 ± 0.05	0.001	0.42 ± 0.06	0.05	6.70 ± 0.33	7.39 ± 0.49	0.001	7.10 ± 0.35	0.01
Precentral WM L	0.45 ± 0.05	0.38 ± 0.05	0.001	0.42 ± 0.07	ns	6.88 ± 0.31	7.24 ± 0.54	0.05	7.10 ± 0.41	0.05
SC-PLIC R	0.57 ± 0.04	0.54 ± 0.04	0.05	0.55 ± 0.05	ns	6.61 ± 0.22	6.97 ± 0.35	0.01	6.93 ± 0.41	0.01
SC-PLIC L	0.58 ± 0.04	0.56 ± 0.05	ns	0.55 ± 0.03	ns	6.64 ± 0.29	6.87 ± 0.34	ns	6.85 ± 0.43	ns
CP R	0.70 ± 0.04	0.61 ± 0.06	0.001	0.65 ± 0.03	0.001	7.16 ± 0.46	7.43 ± 0.47	ns	7.47 ± 0.50	ns
CP L	0.70 ± 0.04	0.63 ± 0.06	0.001	0.65 ± 0.04	0.001	7.24 ± 0.72	7.38 ± 0.41	0.05	7.68 ± 0.54	0.01
Hemipons R	0.49 ± 0.08	0.44 ± 0.06	ns	0.45 ± 0.08	ns	6.31 ± 0.68	6.36 ± 0.63	ns	6.81 ± 0.81	0.05
Hemipons L	0.51 ± 0.09	0.45 ± 0.06	ns	0.44 ± 0.08	0.05	6.45 ± 0.69	6.56 ± 0.61	ns	6.78 ± 0.71	ns
BP R	0.37 ± 0.07	0.30 ± 0.04	0.01	0.33 ± 0.07	ns	9.68 ± 2.72	9.25 ± 2.35	ns	10.06 ± 2.88	ns
BP L	0.37 ± 0.05	0.29 ± 0.04	0.001	0.32 ± 0.06	0.05	9.49 ± 2.42	9.86 ± 2.27	ns	9.19 ± 2.28	ns
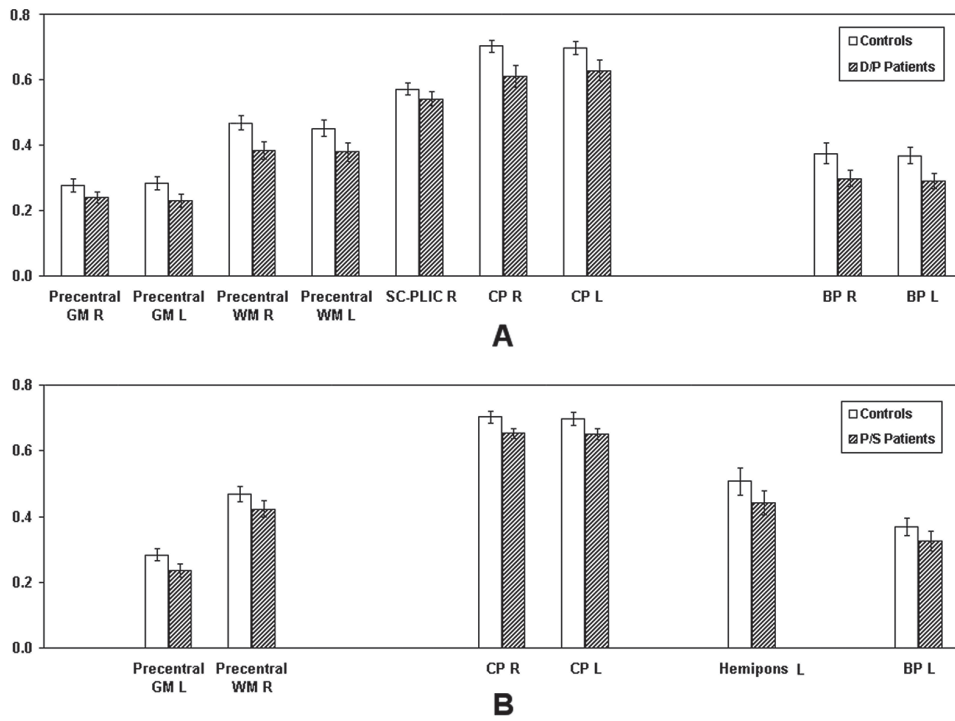
Fig. 1. - Mean FA values and 95% confidence intervals in selected anatomical areas of D/P (A) and P/S ALS patients (B) *vs.* controls.
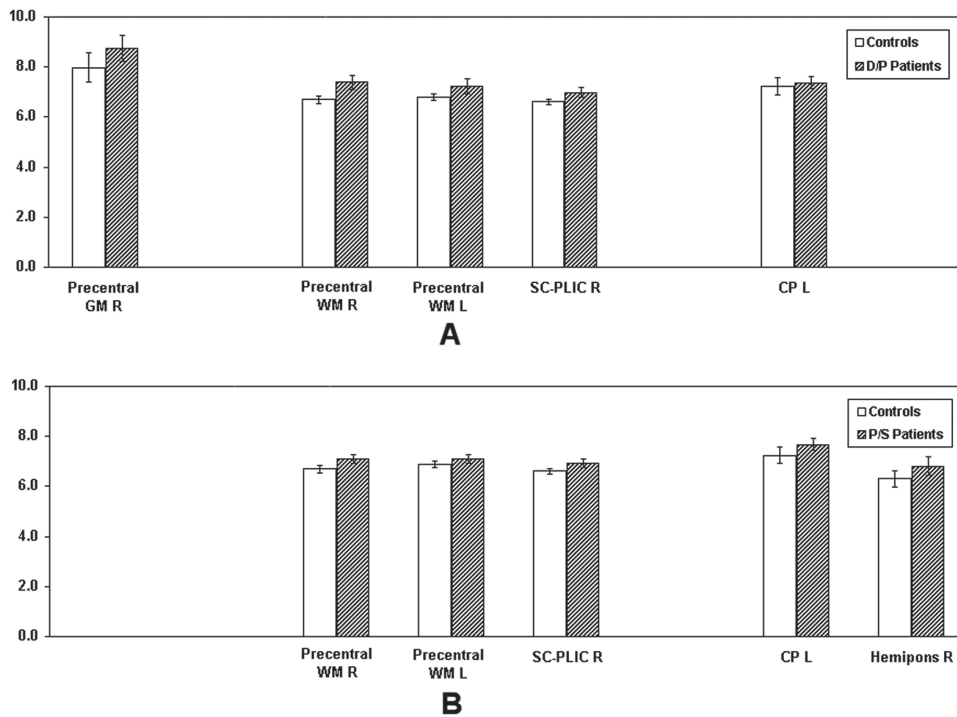

Fig. 2. - Mean avADC values and 95% confidence intervals in selected anatomical areas of D/P (A) and P/S ALS patients (B) *vs.* controls.
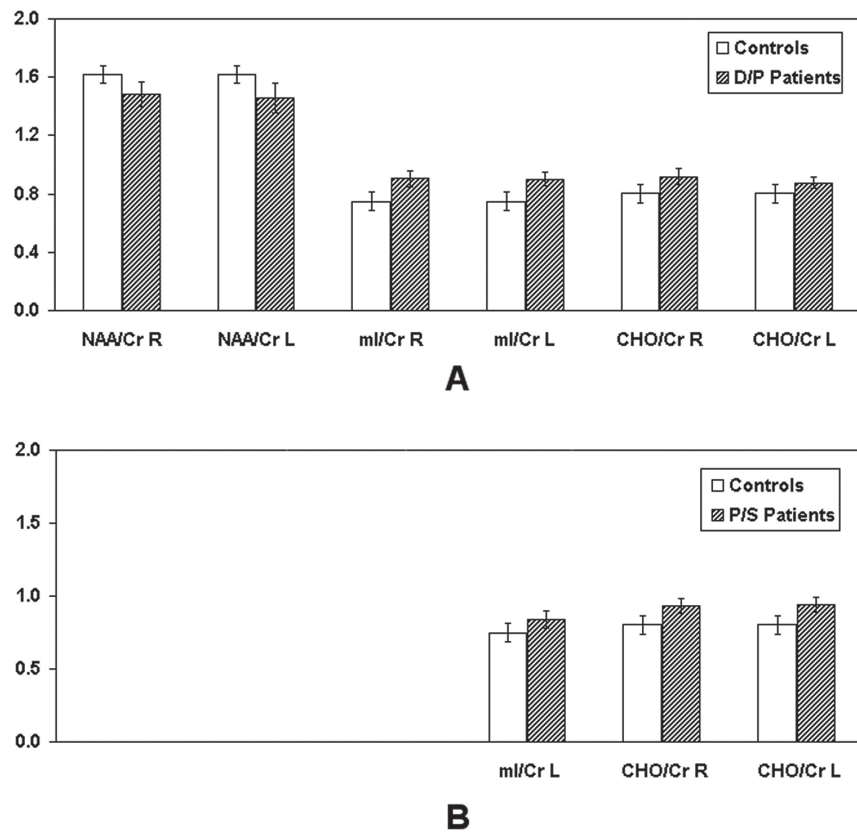
Fig. 3. - Mean NAA/Cr, Cho/Cr and mI/Cr ratios, and 95% confidence intervals in precentral areas of D/P (A) and P/S ALS patients (B) *vs.* controls. Only mean values related to significant differences between subject groups are reported.

Table III. - Means ± standard deviations and statistically significant p-values (if not = ns) for MRS measurements in ASL D/P and P/S patients, and controls.

	Controls n = 19		D/P Patients n = 13	p < values	P/S Patients n = 19	p < values
NAA/Cr	1.62 ± 0.12	R	1.48 ± 0.15	0.05	1.58 ± 0.14	ns
		L	1.46 ± 0.18	0.05	1.58 ± 0.16	ns
mI/Cr	0.75 ± 0.14	R	0.9 ± 0.1	0.01	0.83 ± 0.13	ns
		L	0.9 ± 0.09	0.01	0.84 ± 0.13	0.05
Cho/Cr	0.8 ± 0.14	R	0.92 ± 0.1	0.05	0.93 ± 0.11	0.01
		L	0.88 ± 0.07	0.05	0.94 ± 0.11	0.01

By subdividing patients into groups according to their disability, in Group III PALS compared to Groups I and II, FA mean values tended to be lower in the precentral WM, SC-PLIC and pons, with significance only on the right-hand side ($p < 0.05$). Moreover, in PALS Group III compared to Groups I and II avADC, mean values tended to be higher bilaterally in precentral WM and SC-PLIC, with significance only on the right-hand side ($p < 0.05$). No significant correlation was found between disease severity and spectroscopic data (data not shown).

Disease progression

In D/P-PALS with faster disease progression higher avADC mean values were found in the left precentral GM ($p < 0.05$) and right SC-PLIC ($p < 0.05$) (Fig. 6).
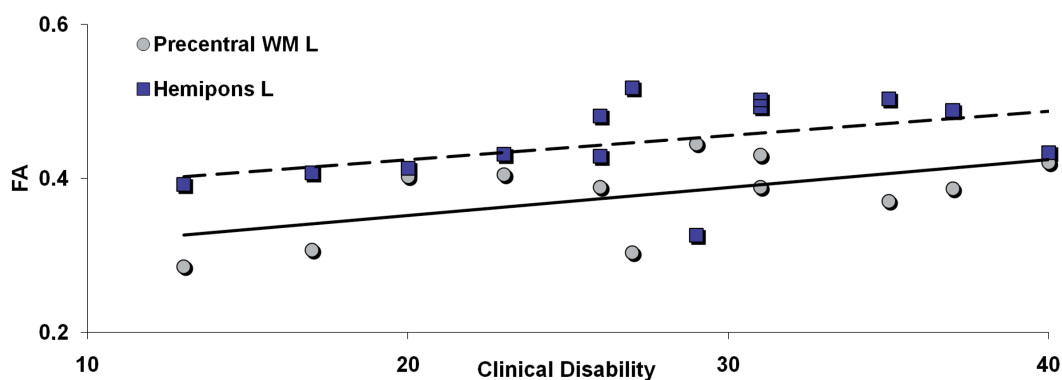
Fig. 4. - Correlation between mean FA and clinical disability in ALS D/P patients.
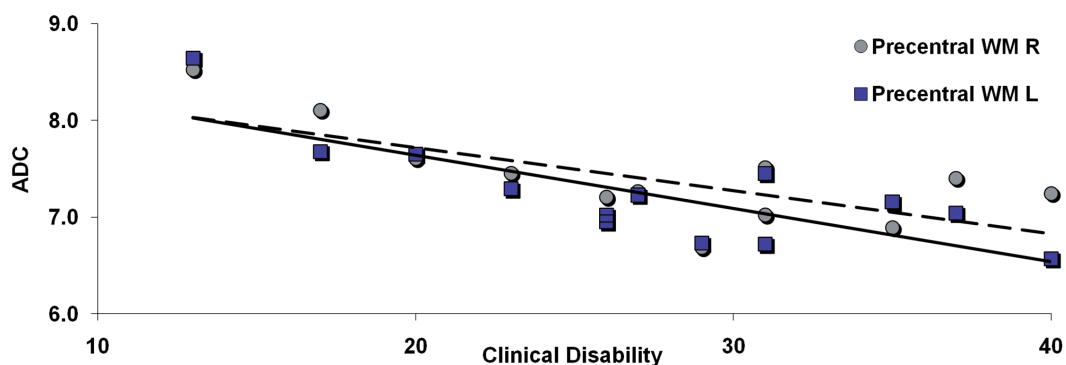

Fig. 5. - Correlation between mean avADC and clinical disability in ALS D/P patients.

FA and spectroscopy data were not found to be significantly different (data not shown).

Sensitivity and specificity

Data sensitivity and specificity were calculated for each anatomical site in which significantly different DTI or H-MRS mean values were found between D/P-PALS and controls. We did not take the P/S-PALS group into account compared to healthy subjects, as it was felt that the diagnostic efficiency of our MRI techniques could only be reliably tested on patients who were most likely affected by ALS. Table IV shows results of the statistical tests that performed well based on the predetermined cut-off value.

Discussion

In 9 (5 males and 4 females; 6 D/P and 3 P/S) of 32 PALS studied, we observed high signals in conventional MRI scans in the CST on T2 or FLAIR images. Our results parallel those from previous authors who claimed that CST hyperintensity is not specific for ALS, because vitamin B12 deficiency, ischemic disease and Friedrich's ataxia may also cause similar MRI findings (Miaux et al., 1994; Peretti-Viton et al., 1999).

The poor sensitivity of qualitative MRI has led to an interest in DTI and H-MRS as quantitative markers of ALS.

Findings outlined in the literature are heterogeneous and sometimes discordant. This might be due to the different anatomical sites explored and methods
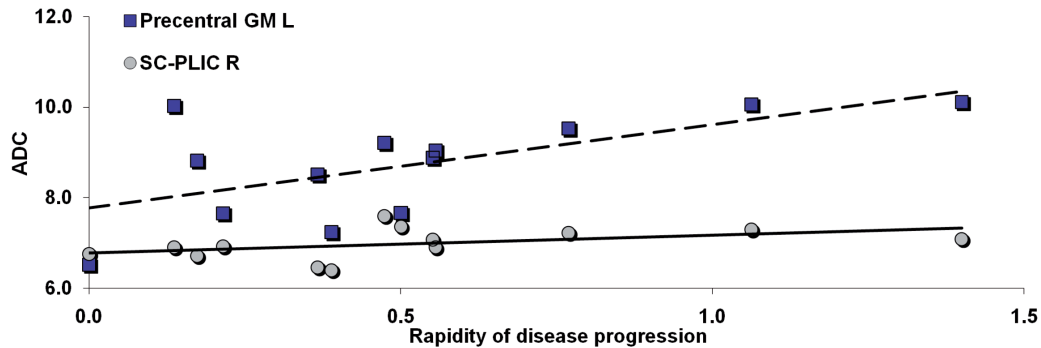
Fig. 6. - Correlation between rapidity of disease progression and mean avADC values in ALS D/P patients.

Table IV. - Sensitivity and Specificity in the anatomical regions in which a statistical significance were found comparing D/P PALS and healthy subjects.

Region of interest	AUC	Sensitivity	Specificity
		FA	
Precentral GM L	88.3	76.9	89.5
Precentral WM R	89.5	84.6	84.2
Precentral WM L	84.4	76.9	84.2
CP R	92.7	92.3	89.5
CP L	85	92.3	78.9
Bulbar Pyramid R	84	61.5	79
Bulbar Pyramid L	88.3	69.2	89.5
		avADC	
Precentral WM R	90.3	76.9	89.5

used (largely ROI; some voxel-based morphometry and probabilistic tractography for ROI placement on the CST or for the calculation of a voxel-based connectivity index). However, it might also depend on the differing clinical features of the PALS selected: for instance, illness duration, which might lead to different histopathological combinations of motor neuron loss, a dysfunction of surviving motor neurons, fiber degeneration, increased extracellular matrix, and glial cell proliferation (Chou and Huang, 1988; Leigh et al., 1989).

We studied motor tracts from the precentral GM to BP$_s$. Only Sach et al. (2004) and Thivard et al. (2007) have previously investigated motor tracts as thoroughly as we did: however, they used a different method from the ROI approach. On the other hand, our study also differs from previous research works, in terms of the higher number of ROI$_s$ located in consecutive slices for each anatomical site. This

means that our measurements achieved a greater statistical power, thus compensating for the objective limitations of using ROI$_s$, such as the so-called "partial volume effect (PVE)" at the level of the precentral GM and bulb, where there are additional complications related to fiber crossing.

None of the previous studies using the "ROI method" examined primary motor GM, probably because of the difficulties in analysing such an anatomical zone that is so superficial and contiguous to rolandic cleft CSF. PVE are in fact responsible for overestimating avADC and underestimating FA values in brain parenchyma (Kwong et al., 1991; Papadakis et al., 2002).

Despite these limitations, cortical GM has been studied using ROI$_s$ in healthy subjects as well and in those with other neurological diseases (Zacharopoulos et al., 1998; Vrenken et al., 2006).

In our study, however, FA underestimation and

avADC overestimation would in any case be reproduced in both PALS and controls, thus cancelling both effects and allowing an adequate comparison between the groups of subjects. We tried to limit PVE by locating individual ROI$_s$ so as to include not only GM, but also part of the precentral WM, nevertheless excluding the central cleft CSF. This means of course that the diffusion indices obtained were influenced not only by GM, but also partially by the subcortical WM. Moreover, motor cortex atrophy in ALS brains has to be carefully taken into account, because it could be responsible for a greater PVE in PALS than in healthy controls. Previous MRI studies, however, have not been able to draw clear conclusions, since this phenomenon was reported by some authors (Chang et al., 2005; Kassubek et al., 2005), but not others (Cheung et al., 1995; Ellis et al., 2001; Abrahams et al., 2005). Such an apparent discrepancy could be explained by the different clinical features of patients and the intrinsic heterogeneity of pathological events (Bertrand et al., 1925; Davison, 1941; Brownell et al., 1970; Chou, 1995; Lowe et al., 1997; Ince, 2000). The progressive tissue loss might then counterbalance the "pseudonormalizing" gliosis effect (Chang et al., 2005). Agosta et al. (2007), using covariance analysis to compare volumetric measurements, recently found significantly reduced GM density in their PALS group only in the right premotor cortex, left inferior frontal gyrus and superior temporal gyri of both sides. Therefore, given the present discrepancies in the literature, we thought it appropriate to specifically study prerolandic GM.

In any case, specific anatomical regions can be explored using ROI$_s$, with extreme precision, thus limiting neuroradiologist-dependent variations. Our findings of non-significant differences between data from ROI positioning by two independently trained neuroradiologists support this concept.

Lower FA mean values observed in PALS in comparison with healthy controls are probably due to structural disorganization resulting from CST motor fiber degeneration, which is almost global in D/P-PALS. Space between surviving fibers is occupied by partially degenerated tracts, extracellular matrix and glial cells.

The fact that mean values were not significantly reduced in the left SC-PLIC and pons of D/P-PALS probably depends on the non-uniformity of histo-pathological lesions which could lead to a lack of significance only in these sites; moreover, as far as pons is concerned, our negative results may be due to crossfibers and nuclei that 'muddle' the selective study of motor CST.

The changes in avADC that we observed may depend on balancing the contrasting effects of different histopathological alterations. An increased extracellular matrix is responsible for an increase in avADC. On the other hand, the latter is reduced by astrocytosis in inter-axonal spaces and debris from nerve fiber degeneration along the CST, which hinder water molecule diffusion (Toosy et al., 2003).

Higher avADC values in precentral regions and right SC-PLIC found in our D/P-PALS, and in the precentral WM, right SC-PLIC and right hemipons, and the left CP found in P/S-PALS can be explained by an increased extracellular volume due to neuronal death and/or reduced neuron size, or axon thinning and/or loss which are not sufficiently compensated by concomitant gliosis (as probably still occurs in all the remaining regions). Variability of statistically significant anatomical sites probably depends on the different combination of histopathological lesions.

Of the two diffusion indices, in D/P-PALS FA is certainly the one which is most commonly altered. Unlike most other authors, we found a significant correlation between the clinical disability of D/P-PALS and both diffusion indices in some of the anatomical sites studied. We have not however, managed to establish whether FA or avADC is the most representative.

On the other hand, only finding significance in some anatomical sites in D/P-PALS with a more rapid disease progression and higher avADC values probably means that avADC is the most reliable diffusion marker in cases with a greater and more rapid motor neuron loss, and thus a reduced number of descending fibers with a consequent extracellular matrix increase.

It is important to note that these conclusions so far are plausible, but purely speculative. Compared to most previous studies, the stronger correlation we found between diffusion indices, patient group and clinical markers probably depends on the different features of the patients enrolled (illness duration, clinical disability, disease progression). In fact, our patients had a higher mean disease duration compared to patients from previous studies. This

would seem to indicate that our subjects had time to develop greater damage to CST. The clinimetric scales used probably play an important role since they are unable to adequately discriminate between disability caused by UMN involvement from that due to LMN involvement. On the other hand, autoptic findings have highlighted a lack of CST involvement (Lawyer et al., 1953; Brownell et al., 1970) in PALS with severe disability.

Our findings probably means there was less CST damage in the P/S than the D/P group. Considering that P/S-PALS also have a long lasting illness which overlaps with D/P-PALS, it would seem to indicate that the former are a subgroup with specific characteristics rather than patients who necessarily become D/P-PALS.

A separate assessment of the S group enabled us to identify DTI parameters consistent with CST damage, but only in a few anatomical sites. This is in agreement with autoptic findings of intracranial CST degeneration in patients who throughout their life showed clinical involvement of just LMN (Ince et al., 2003). We can therefore hypothesize that DTI is more sensitive than a clinical assessment in identifying UMN involvement in S-PALS. This then allows an earlier treatment with riluzole, a neuroprotective glutamatergic inhibitor, which has been proven to modestly extend the survival of PALS (Miller et al., 2003), in accordance with the "National Institute for Clinical Excellence" (NICE, 2003) recommendations. Our observations in this patient subgroup, which parallel those of Graham et al. (2004), would seem to indicate that these patients too could benefit from the riluzole therapeutic effect. Obviously, more cases need to be studied, but if these data are confirmed it would imply that the current prescribing guidelines of riluzole therapy need revisiting.

Using H-MRS, we observed a decreased NAA/Cr ratio and increased mI/Cr and Cho/Cr ratios in D/P-PALS.

The reduced NAA/Cr ratio that we found could be regarded as a marker for motor neuron loss and/or, at least partially, for neuro-axonal dysfunction (Demougeot et al., 2001). However, the single-voxel technique does not allow an adequate distinction between what occurs in GM or subcortical WM. Moreover, some authors have shown that in PALS treated with riluzole there is an increase in NAA/Cr ratios, which could indicate an improvement in

functionality of stressed, but not yet lost, neurons (Karla et al., 1999).

On the assumption that Cho and Cr are ubiquitously present in brain neurons and glial cells (Karla et al., 2003) and that the latter essentially contain no NAA, but high amounts of ml, the increased mI/Cr and Cho/Cr values we found, in agreement with previous studies (Block et al., 1998; Bowen et al., 2000), probably indicate concomitant astrogliosis and a greater membrane phospholipids turnover, respectively, which are known to occur in PALS CST.

Finally, we observed an increased Cho/Cr ratio bilaterally in P/S-PALS and mI on the left-hand side only. We analysed a subgroup of S patients and found increased mI/Cr and Cho/Cr ratios only on the right-hand side. These data parallel those from DTI techniques insofar as they indicate damage in precentral regions, but are less prominent than in D/P-ALS patients.

We did not find any correlation between single metabolite ratios and clinical markers.

Our measurements are not based on metabolite absolute values, but on the ratios between them, on the assumption that there is a good stability of Cr values. Neuronal loss in any case is compensated for by increased reactive astrogliosis. Although a determination of absolute values of metabolites would intuitively be more precise (Lara et al., 1993; Husted et al., 1994; Soher et al., 1996). On the other hand, the use of ratios improves controls on the PVE due to CSF containing only very low metabolite concentrations. Absolute NAA measurements might in fact highlight its decrease in relation to cortical atrophy (Rooney et al., 1998).

Conclusions

Our data highlight that DTI, more than H-MRS, can be useful in assessing UMN involvement in PALS. In fact, by comparing DTI and H-MRS performances, we found that only DTI indices correlate with disease severity and/or progression, showing that the H-MRS technique seems to be less sensitive than DTI. Although ALS diagnosis continues to be largely clinical and electrophysiological, our research, in addition to previous studies, indicates that non-conventional MR techniques may give a better patient characterization, thus allowing riluzole

therapy to be started earlier. In terms of sensitivity and the diagnostic specificity of the diffusion index calculation in D/P-PALS, despite the small sample size, our findings on FA are encouraging and help support its use as diagnostic index. MR techniques need to be used on larger samples, and in many different centres, in order to improve their statistical significance with regard to sensitivity and diagnostic specificity. However, it would seem reasonable to state that DTI and H-MRS enable us to select and monitor PALS in clinical trials more effectively and more precisely.

References

Abrahams S., Goldstein L.H., Suckling J., Ng V., Simmons A., Chitnis X., Atkins L, Williams SC, Leigh PN. Frontotemporal white matter changes in amyotrophic lateral sclerosis. *J. Neurol.*, **252**: 321-331, 2005.

Agosta F., Pagani E., Rocca M.A., Caputo D., Perini M., Salvi F., Prelle A., Filippi M. Voxel-based morphometry study of brain volumetry and diffusivity in amyotrophic lateral sclerosis patients with mild disability. *Hum. Brain Mapp.*, **28** (12):1430-1438, 2007.

Bertrand I. and Van Bogaert L. La sclerose laterale amyotrophique (anatomie pathologique). *Rev. Neurol.*, **25**: 779-806, 1925.

Blain C.R., Williams V.C., Johnston C., Stanton B.R., Ganesalingam J., Jarosz J.M., Jones D.K., Barker G.J., Williams S.C., Leigh N.P., Simmons A. A longitudinal study of diffusion tensor MRI in ALS. *Amyotroph. Lateral Scler.*, **8** (6): 348-355, 2007.

Block W., Karitzky J., Treaber F., Pohl C., Keller E., Mundegar R.R., Lamerichs R., Rink H., Ries F., Schild H.H., Jerusalem F. Proton magnetic resonance spectroscopy of the primary motor cortex in patients with motor neuron disease: subgroup analysis and follow-up measurements. *Arch. Neurol.*, **55**: 931-936, 1998.

Bowen B.C., Pattany P.M., Bradley W.G., Murdoch J.B., Rotta F., Younis A.A., Duncan R.C., Quncer R.M. MR imaging and localized proton spectroscopy of the precentral gyrus in amyotrophic lateral sclerosis. *AJNR Am. J. Neuroradiol.*, **21**: 647-658, 2000.

Brooks B.R., Miller R.G., Swash M., Munsat T.L. El Escorial revisited: revised criteria for the diagnosis of amyotrophic lateral sclerosis. *Amyotroph. Lateral Scler. Other Motor Neuron. Disord.*, **1**: 293-299, 2000.

Brownell B., Oppenheimer D.R., Hughes J.T. The central nervous system in motor neurone disease. *J. Neurol. Neurosurg. Psychiatry*, **33**: 338-357, 1970.

Cedarbaum J.M., Stambler N. Performance of the Amyotrophic Lateral Sclerosis functional rating-scale (ALSFRS) in multicenter clinical trials. *J. Neurol. Sci.*, **152**: 1-9, 1997.

Chang J.L., Lomen-Hoerth C., Murphy J., Henry R.G., Kramer J.H., Miller B.L., Gorno-Tempini M.L. A voxel-based morphometry study of patterns of brain atrophy in ALS and ALS/FTLD. *Neurology*, **65**: 75-80, 2005.

Cheung G., Gawel M.J., Cooper P.W., Farb R.I., Ang L.C., Gawal M.J. Amyotrophic lateral sclerosis: correlation of clinical and MR imaging findings. *Radiology*, **194**: 263-270, 1995.

Chou S.M. Pathology of motor system disorder. pp. 53-92. In: Leigh P.N., Swash M. (Eds.). *Motor neuron disease: biology and management*. London, Springer-Verlag, 1995.

Chou S.M. and Huang T.E. Giant axonal spheroids in internal capsules of amyotrophic lateral sclerosis brains revisited. *Ann. Neurol.*, **24**: 168, 1988.

Ciccarelli O., Behrens T.E., Altman D.R., Orrell R.W., Howard R.S., Johansen-Berg H., Miller D.H., Matthews P.M., Thompson A.J. Probabilistic diffusion tractography: a potential tool to assess the rate of disease progression in amyotrophic lateral sclerosis. *Brain*, **129**: 1859-1871, 2006.

Cosottini M., Giannelli M., Siciliano G., Lazzarotti G., Michelassi M.C., Del Corona A., Bartolozzi C., Murri L. Diffusion-tensor MR imaging of corticospinal tract in amyotrophic lateral sclerosis and progressive muscular atrophy. *Radiology*, **23**: 258-264, 2005.

Davison C. Amyotrophic lateral sclerosis: origin and extent of upper motor neuron lesion. *Neurol. Psychiatr.*, **46**: 1039-1056, 1941.

Demougeot C., Garnier P., Mossiat C., Bertrand N., Giroud M., Beley A., Marie C. N-Acetylaspartate, a marker of both cellular dysfunction and neuronal loss: its relevance to studies of acute brain injury. *J. Neurochem.*, **7**: 408-415, 2001.

Dixon R.M., Bradley K.M., Budge M.M., Styles P., Smith A.D. Longitudinal quantitative proton magnetic resonance spectroscopy of the hippocampus in Alzheimer's disease. *Brain*, **125**: 2332-2341, 2002.

Ellis C.M., Simmons A., Jones D.K., Bland J., Dawson J.M., Horsfield M.A., Williams S.C.R., Leigh P.N. Diffusion tensor MRI assesses corticospinal tract damage in ALS. *Neurology*, **53**: 1051-1058, 1999.

Ellis C.M., Suckling J., Amaro E. Jr., Bullmore E.T., Simmons A., Williams S.C. Volumetric analysis reveals corticospinal tract degeneration and extramotor involvement in ALS. *Neurology*, **57**: 1571-1578, 2001.

Fernando K.T., McLean M.A., Chard D.T., MacManus D.G., Dalton C.M., Miszkiel K.A., Gordon R. M., Plant G.T., Thompson A.J., Miller D.H. Elevated white matter myo-inositol in clinically isolated syndromes suggestive of multiple sclerosis. *Brain*, **127**: 1361-1369, 2004.

Graham J.M., Papadakis N., Evans J., Widjaja E., Romanowski C.A.J., Paley M.N.J., Wallis L.I., Wilkinson I.D., Shaw P.J., Griffiths P.D. Diffusion tensor imaging for the assessment of upper motor neuron integrity in ALS. *Neurology*, **63**: 2111-2119, 2004.

Gredal O., Rosembaum S., Topp S., Karlsborg M., Strange P., Werdelin L. Quantification of brain metabolites in amyotrophic lateral sclerosis by localized proton magnetic resonance spectroscopy. *Neurology*, **50**: 878-881, 1997.

Hong Y., Lee K., Sung J., Chang K., Song I.C. Diffusion tensor MRI as a diagnostic tool of upper motor neuron involvement in amyotrophic lateral sclerosis. *J. Neurol. Sci.*, **227**: 73-78, 2004.

Husted C.A., Duijn J.H., Matson G.B., Maudsley A.A., Weiner M.W. Molar quantitation of in vivo proton metabolites in human brain with 3D magnetic resonance spectroscopic imaging. *Magn. Reson. Imaging*, **12**: 661-667, 1994.

Ince P.G. Neuropathology. pp. 83-112. In: Brown R.H., Meininger V., Swash M. (Eds.). *Amyotrophic lateral sclerosis*. London, Martin Dunitz, 2000.

Ince P.G., Evans J., Knopp M., Forster G., Hamdalla H.H.M., Wharton S.B., Shaw P.J. Corticospinal tract degeneration in the progressive muscular atrophy variant of ALS. *Neurology*, **60**: 1252-1258, 2003.

Isobe T., Matsumura A., Anno I., Yoshizawaa T., Nagatomo Y., Itai Y., Nose T. Quantification of cerebral metabolites in glioma patients with proton MR spectroscopy using T2 relaxation time correction. *Magn. Reson. Imaging*, **20**: 343-349, 2002.

Iwata N.K., Aoki S., Okabe S., Arai N., Terao Y., Kwak S., Abe O., Kanazawa I., Tsuji S., Ugawa Y. Evaluation of corticalspinal tracts in ALS with diffusion tensor MRI and brainstem stimulation. *Neurology*, **70**: 528-532, 2008.

Kalra S., Arnold D.L., Cashman N.R. Biological markers in the diagnosis and treatment of ALS. *J. Neurol. Sci.*, 165 (Suppl 1): S27-S32, 1999.

Kalra S. and Arnold D. Neuroimaging in amyotrophic lateral sclerosis. *Amyotroph. Lateral Scler. Other Motor Neuron. Disord.*, **4**: 243-248, 2003.

Kalra S., Hanstock C.C., Martin W.R.W., Allen P.S., Johnston W.S. Detection of cerebral degeneration in amyotrophic lateral sclerosis using high-field magnetic resonance spectroscopy. *Arch. Neurol.*, 63: 1144-1148, 2006.

Kassubek J., Unrath A., Huppertz H.J., Lulé D., Ethofer T., Sperfeld A.D., Ludolph AC. Global brain atrophy and corticospinal tract alterations in ALS, as investigated by voxel-based morphometry of 3-D MRI. *Amyotroph. Lateral Scler. Other Motor Neuron. Disord.*, **6**: 213-220, 2005.

Ken W., Ochs G., Pabst T.A., Hahn D. 1H spectroscopy in patients with amyotrophic lateral sclerosis. *J. Neuroimaging*, **11**: 293-297, 2001.

Kwong K., McKinstry R., Chien D., Crawley A., Pearlman J., Rosen B. CSF-suppressed quantitative single-shot diffusion imaging. *Magn. Reson. Med.*, **21**: 157-163, 1991.

Lara R.S., Matson G.B., Hugg J.W., Maudsley A.A., Weiner M.W. Quantitation of in vivo phosphorus metabolites in human brain with magnetic resonance spectroscopic imaging (MRSI). *Magn. Reson. Imaging*, **11**: 273-278, 1993.

Lawyer T. Jr. and Netsky M.G. Amyotrophic lateral sclerosis: a clinico-anatomic study of 53 cases. *Arch. Neurol.*, **69**: 171-192, 1953.

Leigh P.N., Dodson A., Swash M., Brion J.P., Anderton B.H. Cytoskeletal abnormalities in motor neuron disease. An immunocytochemical study. *Brain*, **112**: 521-535, 1989.

Lowe J., Lennox G., Leigh P.N. Disorders of movement and system degenerations. pp. 281-366. In: Graham D.J., Lantos P.L. (Eds.). *Greenfield's neuropathology vol. 2*. London, Arnold, 1997.

Miaux Y., Martin-Duverneuil N., Cognard C., Weill A., Chiras J. Areas of high signal intensity in the posterior limbs of the internal capsules in amyotrophic lateral sclerosis: normal or pathologic MR finding? *Radiology*, **191**: 870-871, 1994.

Miller R.G., Mitchell J.D., Lyon M., Moore D.H. Riluzole for amyotrophic lateral sclerosis (ALS)/ motor neuron disease (MND). *Amyotroph. Lateral Scler. Other Motor Neuron. Disord.*, **4**: 191-206, 2003.

Mitsumoto H., Ulug A.M., Pullman S.L., Gooch C.L., Chan S., Tang M.X., Mao X., Hays A.P., Floyd A.G., Battista V., Montes J., Hayes S., Dashnaw S., Kaufmann P., Gordon P.H., Hirsch J., Levin B., Rowland L.P., Shungu D.C. Quantitative objective markers for upper and lower motor neuron dysfunction in ALS. *Neurology*, **68**: 1402-1410, 2007.

Papadakis N., Martin K., Mustafa M., Wilkinson I.D., Griffiths P.D., Huang C.L.H., Woodruff P.W.R. Study of the effect of the CSF suppression on white matter diffusion anisotropy mapping in healthy human brain. *Magn. Reson. Med.*, **48**: 394-398, 2002.

Peretti-Viton P., Azulay J.P., Trefouret S., Brunel H., Daniel C., Viton J.M., Flori A., Salazard B., Pouget J., Serratrice G., Salamon G. MRI of the intracranial cortico-spinal tracts in amyotrophic and primary lateral sclerosis. *Neuroradiology*, **41**: 744-749, 1999.

Pierpaoli C. and Basser P.J. Toward a quantitative assessment of diffusion anisotropy. *Magn. Reson. Med.*, **36**: 893-906, 1996.

Pohl C., Block W., Karitzky J., Schmidt S., Pels H., Grothe C., Lamerichs R., Schild H.H., Klockgether T. Proton magnetic resonance spectroscopy of the motor cortex in 70 patients with amyotrophic lateral sclerosis. *Arch. Neurol.*, **58**: 714-716, 2001.

Rooney W.D., Miller R.G., Gelinas D., Schuff N., Maudsley A.A., Weiner M.W. Decreased N-acetylaspartate in motor cortex and corticospinal tract in ALS. *Neurology*, **50**: 1800-1805, 1998.

Sach M., Winkler G., Glauche V., Liepert J., Heimbach B., Koch M.A., Buchel C., Weiller C. Diffusion tensor MRI of early upper motor neuron involvement in amyotrophic lateral sclerosis. *Brain*, **127**: 340-350, 2004.

Sage C.A., Peeters R.R., Gorner A., Robberecht W., Sunaert S. Quantitative diffusion tensor imaging in amyotrophic lateral sclerosis. *Neuroimage*, **34**: 486-499, 2007.

Schubert F., Seifert F., Elster C., Link A, Walzel M, Mientus S, Haas J., Rinneberg H. Serial 1H-MRS in relapsing-remitting multiple sclerosis: effects of interferon-beta therapy on absolute metabolite concentrations. *MAGMA*, **14**: 213-222, 2002.

Soher B.J., van Zijl P.C., Duyn J.H., Barker B.P. Quantitative proton MR spectroscopic imaging of the human brain. *Magn. Reson. Med.*, **35**: 356-363, 1996.

Suhy J., Miller R.G., Rule R., Schuff N., Licht J., Dronsky V., Gelinas D., Maudsley A.A., Weiner M.W. Early detection and longitudinal changes in amyotrophic lateral sclerosis by (1)H MRSI. *Neurology*, **58**: 773-779, 2002.

Swets J.A. Measuring the accuracy of diagnostic systems. *Science*, **240**: 1285-1293, 1998.

Thivard L., Pradat P.F., Lehéricy S., Lacomblez L., Dormont D., Chiras J., Benali H., Meininger V. Diffusion tensor imaging and voxel based morphometry study in amyotrophic lateral sclerosis: relationships with motor disability. *J. Neurol. Neurosurg. Psychiatry*, **78**: 889-892, 2007.

Toosy A.T., Werring D.J., Orrell R.W., Howard R.S., King M.D., Barker G.J., Miller D.H., Thompson A.J. Diffusion tensor imaging detects corticospinal tract involvement at multiple levels in amyotrophic lateral sclerosis. *J. Neurol. Neurosurg. Psychiatry*, **74**: 1250-1257, 2003.

Traber F., Block W., Freymann N., Gürl O., Kucinski T., Hammen T., Ende G., Pilatus U., Hampel H., Schild H.H., Heun R., Jessen F. A multicenter reproducibility study of single-voxel 1H-MRS of the medial temporal lobe. *Eur. Radiol.*, **16**: 1096-1103, 2006.

Vrenken H., Pouwels P.J.W., Geurts J.J.G., Knol D.L., Polman C.H., Barkhof F., Castelijns J.A. Altered diffusion tensor in multiple sclerosis normal-appearing brain tissue: cortical diffusion changes seem related to clinical deterioration. *J. Magn. Reson. Imaging*, **23**: 628-636, 2006.

Wang S., Poptani H., Woo J.H., Desiderio L.M., Elman L.B., McCluskey L.F., Krejza J., Melhem E.R. Amyotrophic lateral sclerosis: diffusion tensor and chemical shift MR imaging at 3.0 T. *Radiology*, **239**: 831-838, 2006.

World Federation of Neurology Research Group. El Escorial World Federation of Neurology Criteria for the Diagnosis of Amyotrophic Lateral Sclerosis. *J. Neurol. Sci.*, **124** (Suppl): 96-107, 1994.

Yin H., Lim C.C.T., Ma L., Gao Y., Cai Y., Li D., Liang Y., Guo X. Combined MR spectroscopic imaging and diffusion tensor MRI visualizes corticospinal tract degeneration in amyotrophic lateral sclerosis. *J. Neurol.*, **251**: 1249-1254, 2004.

Zacharopoulos N. and Narayana P. Selective measurement of white matter and gray matter diffusion trace values in normal human brain. *Med. Phys.*, **25**: 2237-2241, 1998.